Structural investigation of *a*-Si and *a*-Si:H using x-ray-absorption spectroscopy at the Si *K* edge

A. Filipponi and F. Evangelisti
Departimento di Fisica, Prima Università degli Studi di Roma La Sapienza, piazzale Aldo Moro 2, I-00185 Roma, Italy

M. Benfatto, S. Mobilio, and C. R. Natoli
Laboratori Nazionali di Frascati dell'Istituto Nazionale della Fisica Nucleare, Casella Postale 13, I-00044 Frascati, Italy

(Received 18 January 1989; revised manuscript received 24 July 1989)

X-ray-absorption spectra of *a*-Si and *a*-Si:H at the Si *K* edge are reported. By means of a nonstandard data-analysis procedure, we show that the fine-structure spectrum contains, besides the first-shell single-scattering extended x-ray-absorption fine-structure (EXAFS) signal, a higher-frequency contribution as well. Very accurate first-shell distances, coordination numbers, and mean-square relative displacements are obtained for all amorphous samples. The residual high-frequency signal is correctly reproduced only if multiple-scattering effects due to three-body correlations are taken into account. This result shows that x-ray-absorption spectroscopy has the potentiality for probing structural information beyond the pair correlation function in amorphous systems.

I. INTRODUCTION

The structure of *a*-Si has been extensively investigated by means of x-ray-scattering[1,2] and elastic-neutron-scattering techniques,[3] and its pair correlation function $g_2(r)$ is known up to about 10 Å. Several theoretical models[4–8] have been recently developed that are based on the continuous random network[9,10] and able to reproduce satisfactorily the $g_2(r)$. In order to characterize in a better way the three-dimensional structure of *a*-Si, experimental structural information beyond the pair correlation function like the three-body correlation function would be of particular interest.

An alternative determination of the structure is achieved by means of the x-ray-absorption spectroscopy (XAS), which provides a local picture of the surrounding of a particular atom. In monoatomic compounds, like *a*-Si, the use of extended x-ray absorption fine structure[11] (EXAFS) allows the determination of the total pair correlation function and in particular of the first-shell structural parameters, with high accuracy.

Besides, EXAFS is not the only signal present in x-ray-absorption spectra, since other contributions are present as well, mainly in the so-called x-ray-absorption near-edge structure (XANES) region.[12,13] The multiple-scattering theory of the x-ray-absorption coefficient shows that such contributions are related to correlation functions of order higher than 2. Therefore, in principle XAS can give structural information not obtainable with x-ray- and neutron-diffraction experiments. However, up to now there are no instances of higher-order correlation effects being detected in an x-ray-absorption spectrum of disordered systems.

Many EXAFS investigations on *a*-Si and *a*-Si:H have been reported, dealing mainly with the study of the first shell.[14–16] All these papers did not take into account the presence of a multielectron excitation at about 124 eV above the Si *K* absorption edge, which affects the shape of the EXAFS spectrum, introduces an unphysical peak in the Fourier transform[17] and therefore affects the determination and the accuracy of the first-shell structural parameters. Moreover, no previous author has attempted to investigate quantitatively the region beyond the nearest neighbors.

In the present paper we report very-low-noise spectra of *a*-Si and *a*-Si:H at different H content. Taking into account the presence of the multielectron excitation, we have analyzed the spectra using a nonconventional procedure. We show that apart from the first-shell EXAFS, an additional high-frequency signal contributes to the spectra. This signal can be reproduced only if several multiple-scattering terms involving the second shell and the three-body correlation function are taken into account.

II. EXPERIMENT

Two samples of *a*-Si:H were deposited by glow-discharge in SiH_4 on a 12.5-μm-thick Be foil. Substrate temperature and chamber pressure were 250 °C an 0.8 Torr for one sample and 80 °C and 0.2 Torr for the other. The hydrogen content of the samples was measured by infrared spectroscopy integrating the Si-H wagging mode at 640 cm^{-1} and resulted to be 14% and 21%, respectively. A sample of a pure *a*-Si was grown on a substrate held at room temperature using dual–ion-beam sputtering technique. All amorphous samples were characterized using ir and optical spectroscopy. A microcrystalline silicon sample, prepared by recrystallizing an *a*-Si film, was used as a reference compound.

X-ray-absorption spectra were taken using the x-ray beam line of the ACO storage ring at the LURE synchrotron radiation facility (Orsay, France). The incoming beam was monochromatized using an InSb(111) double crystal monochromator. The spectra were recorded in the energy region 1800–2300 eV with a step of 1 eV and an integration time of ≈ 2 s. The beam intensity was measured by a single ion chamber located after the sample. To normalize the spectra, the incoming radiation I_0 was monitored every two sample measurements. Several spectra for each sample were taken and averaged, in order to obtain final spectra of high quality with a signal-to-noise ratio of the order of 10^4.

III. DATA ANALYSIS

In a previous paper[17] it was shown that a two-electron channel (*KL* edge) contributes appreciably to the absorption, starting at ≈ 124 eV above the Si *K* edge. The standard EXAFS analysis procedures do not take into account this *KL* absorption edge, and therefore provide distorted spectra.

Moreover, in the Fourier algorithm generally used to process the data, the side lobes associated with the main signals in the spectra distort possible smaller contributions and prevent their quantitative analysis. It has been shown that in order to reveal and analyze such small contributions a better approach is to break up the absorption spectra in terms of partial contributions.[13] For these reasons we have processed our spectra with a nonconventional data analysis, working directly on the absorption spectra. The basic ideas of the procedure have been already described;[17] however, they are repeated here for completeness. We consider each absorption spectrum as composed of three contributions: (a) an atomic *K*-edge cross section plus a smooth background; (b) a *KL*-edge contribution which gives rise to a sudden jump in the absorption at ≈ 1960 eV; (c) the EXAFS signals due to the various coordination shells.

Therefore, we have chosen to fit to the absorption coefficient a model signal composed of three parts: (a) a smooth polynomial spline; (b) a step function with a jump of variable height at 1960 eV; (c) the sum of a number of oscillating EXAFS-like signals with smooth, *k*-dependent, amplitudes and phases properly parametrized.

The experimental EXAFS spectrum is defined as the difference between the absorption spectrum and the total atomic background signals $a+b$, normalized as usual[18] by $J[1-8(E-E_0)/3E_0]$; here J is the *K*-edge discontinuity and E_0 its energy position. This definition coincides with the usual one, provided the *KL*-edge contribution is taken into account. The oscillating EXAFS-like contributions (c) are written as

$$\chi(k)=\sum_j N_j/(kR_j^2)f_j(k,\pi)\exp(-2\sigma_j^2k^2) \times\exp(-2R_j/\lambda)\sin[2kR_j+\phi_j(k)] .$$

The sum extends over the various shells surrounding the central atom and R_j, N_j, and σ_j^2 are, respectively, the distances, the coordination numbers, and the variances of each shell distance. The phase $\phi_j(k)$ and amplitude $f_j(k,\pi)$ were parametrized as

$$\phi_j(k)=F_0+F_1k+F_2k^2$$

and

$$f_j(k,\pi)=(A+D/k^2)/[B+(k-C)^2] .$$

A similar parametrization has been used by Teo and Lee[19] and describes appropriately the theoretical phases at least in the plane-wave approximation. We have verified by actual calculations that in the energy range used for the fittings such a parametrization can reproduce the total phase and backscattering functions in the spherical wave approximation too. The mean-free-path term $\exp(-2R_j/\lambda)$ present in the above expression was ignored during all the fittings, since a comparative analysis between similar systems was performed so that the mean-free-path term is expected to be the same and included in the $f_j(k,\pi)$.

The analysis proceeds according to the well-known phase[20] and amplitude[21] transferability: first the backscattering amplitude $f_j(k,\pi)$ and phase function $\phi_j(k)$ are fitted on the spectrum of the model compound with known structure and the coefficients F_0,F_1,F_2,A,B,C,D are determined. Then these functions are used in fitting the spectra of the materials with unknown structure. In such a case N_j, R_j, and σ_j^2 become fitting parameters. In the last step, a possible shift of the energy scale is also included.

In our specific case, the *a*-Si:H with 14% of H was used as a model for the first-shell phase and amplitude. The reason for this choice was twofold: first of all the spectra of the amorphous samples had a considerably better signal-to-noise ratio than the spectrum of *c*-Si. Moreover, in the amorphous samples the signal is mainly due to the first shell so that a single-shell fitting provides reliable parameters for the first-shell phase and amplitude. We did not use the *c*-Si as a model since in this sample the presence of single- and multiple-scattering contributions to the signal from shells higher than the first makes a single-shell fitting unreliable.[22] A multishell fitting, on the other hand, needs an overly large number of parameters. Amplitude and phase functions so obtained were then used to fit the spectra of *a*-Si:H (21%) and *a*-Si samples. This procedure allowed us to perform a very accurate comparative analysis among the amorphous samples.

It was already established[23] that the EXAFS signal due to the first shell is not the only one present in the amorphous spectra: a "residual" high-frequency oscillation was noticed, which amounts to about 5–10 % of the total signal. It is clear that this residual signal contains information on the second coordination shell, but up to now its origin and nature has not been completely investigated. To account for its presence we have reiterated the analysis with a further oscillating contribution added to the component (c) of the model signal of all amorphous spectra. The final fittings provided model signals practically indistinguishable from the experimental spectra as clearly seen in Fig. 1. The values of the structural param-

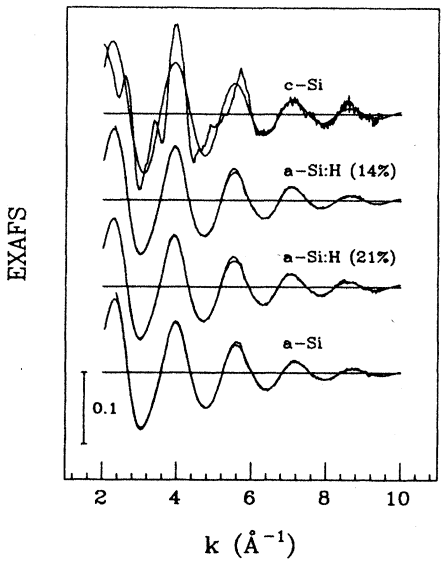

FIG. 1. Experimental EXAFS spectra of *c*-Si, *a*-Si, and *a*-Si:H samples. The smooth solid curves which interpolate the data are best-fitting spectra obtained as discussed in the text, with a one-shell fitting for *c*-Si and two-shell fitting for amorphous samples. The one-shell fittings for the amorphous samples differ only slightly on this scale and therefore are not shown.

eters obtained for the first shell did not change as compared to the values obtained in the previous analysis.

In order to have an absolute calibration for the structural parameters, the model amplitude and phase were also used to fit the first-shell contribution in the *c*-Si spectrum (Fig. 1). The discrepancy shown in the figure is obviously due to the presence of higher shells and multiple-scattering contributions in the experimental spectrum. In this way an absolute calibration was obtained which, however, for the reason explained above, is less accurate than the relative comparison between the amorphous samples.

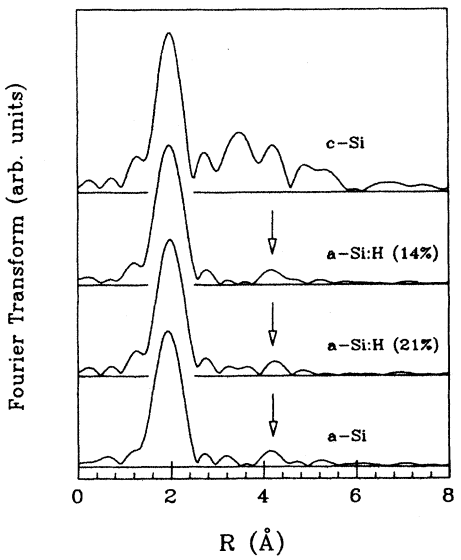

FIG. 2. Fourier transforms of the experimental EXAFS spectra of Fig. 1. The presence of a weak high-frequency signal in the amorphous spectra is evidenced by arrows.

The Fourier transforms (FT's) of the experimental EXAFS spectra, performed in the k interval 2.2–9.5 Å^{-1} with a weight k^2 and a Hanning window 0.5 Å wide, are reported in Fig. 2. In all the FT's the first-shell peak appears as an isolated peak with symmetric side lobes. No trace is left of the peak at 1.3 Å, generally present in all the FT's of *K*-edge silicon spectra, due to the distortion introduced by the *KL*-edge transition.[17]

At the same time in the FT's of the amorphous samples a further peak at $\approx$4.2 Å is also present, which originates from the above-mentioned high-frequency residual. The R position of this peak does not coincide with the second shell of *c*-Si, which occurs at 3.84 Å minus the phase-shift contribution of $\approx$0.35 Å. Instead its position seems to coincide with the "third-shell" *c*-Si peak. This coincidence can be fortuitous, because in silicon the oscillation frequency of the second- and third-shell overlap with those of several multiple-scattering paths.[23]

IV. RESULT AND DISCUSSION

A. The first shell

In Table I we report the results obtained for the first-shell coordination number, bond length, and σ_j^2. The absolute values of the structural parameters have been obtained through the above-mentioned procedure. The values of *c*-Si are also reported for comparison; its σ_j^2 at 300 K has been calculated using the high-temperature expansion for the vibrational correlation function.[24] The values reported are in good agreement with our previous investigation,[16] but the accuracy obtained here is higher.

Let us first comment on the results on the coordination number. From the data we find that Si atoms in the amorphous hydrogenated samples are undercoordinated with respect both to the *a*-Si and *c*-Si samples. This undercoordination is due to the presence of Si—H bonds

TABLE I. First-shell coordination number N_0, average distance R_j, and variance σ^2, of the various samples. The last column reports the H concentration as deduced using Eq. (1) of the text, assuming as a reference the *a*-Si coordination. The errors reported refer to the absolute calibration. As discussed in the text the errors of the differences among the amorphous samples are smaller and amount to 1% for the coordination and 0.4×10^{-3} Å^2 for the σ^2.

Sample	$N_c/4$	R (Å)	σ^2 (10^{-3} Å^2)	[H] (%)
c-Si	1	2.352	3.4	
a-Si:H (14%)	0.97(3)	2.35(1)	4.4(8)	8%
a-Si:H (21%)	0.92(3)	2.36(1)	3.9(8)	22%
a-Si	0.99(3)	2.36(1)	5.6(8)	0%

not seen by EXAFS. In the hypothesis of a negligible effect coming from dangling bonds and from voids, it is possible to evaluate the hydrogen concentration [H] from the silicon coordination as:[2]

$$[\mathrm{H}]=(4-N_c)/(5-N_c)\ . \tag{1}$$

The values obtained, reported in the last column of Table I, are in good agreement with the ir data.

As for the bond lengths, the Si-Si distance does not show meaningful differences among the various samples confirming previous results. On the other hand, differences in the σ_j^2 are found. All amorphous samples are more disordered than the crystal as a consequence of the distribution in the equilibrium bond length. Moreover, we found a larger σ_j^2 in a-Si than in the hydrogenated samples: the incorporation of H during glow-discharge deposition results in a material whose intrinsic disorder is smaller than that in the sputtered a-Si.

B. High-frequency residue signals and multiple-scattering calculations

The "high-frequency" residual signals, shown in Fig. 3, are obtained by subtracting from the experimental EXAFS spectra the first-shell model contribution. The region around the KL edge is reported with a dotted line because it is less reliable than the other part of the signal. Indeed the line shape of the KL threshold could not be well described by the model we used to account for it. The amplitude of the high-frequency residual is of the order of 10^{-2}; therefore it contributes 5–10 % to the total oscillating fine-structure signal and its intensity is well above the noise level of our spectra.

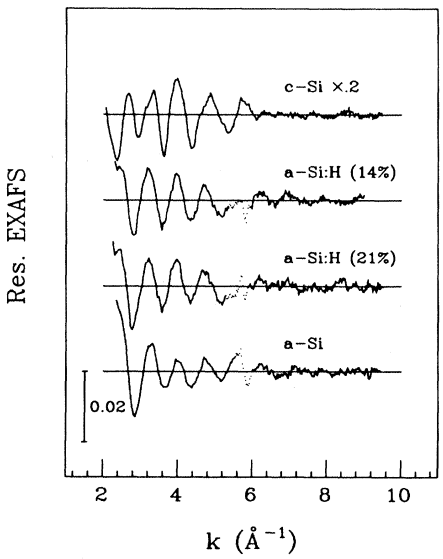

FIG. 3. Residual high-frequency signals beyond the first-shell EXAFS. The c-Si spectrum has been divided by a factor of 5 for graphical convenience.

Note that the two hydrogenated samples have very similar residual signals, but show differences from c-Si in all the k range. Also the a-Si:H and a-Si samples have different residuals, that is, although the leading frequency is the same, the amplitude of the residual in the a-Si spectrum is on the average smaller, especially around 4 Å^{-1}. This is again evidence of a structural difference between our a-Si and a-Si:H samples.

A full quantitative interpretation of these high-frequency residuals cannot be obtained within the framework of the single-scattering formula; indeed many multiple-scattering paths contribute appreciably to the spectra in that frequency region. We have therefore performed a multiple-scattering calculation within the following theoretical framework.

As is known,[12,13] above some particular energy the absorption coefficient of a K edge is given by the following series expansion:

$$\alpha(k)=\alpha_0\sum_n \chi_n^l(k)$$

$$=\alpha_0\sum_n \frac{(-1)^n}{3\sin^2\delta_{0l}}\sum_m \mathrm{Im}\{[(T_A G)^n T_A]^{0,0}_{lm,lm}\}\ . \tag{2}$$

In this expression α_0 is the atomic absorption coefficient, l is the photoelectron final-state angular momentum (equal to 1 in the present case), δ_{0l} is the l-wave phase shift of the absorbing atom located at the origin, G is the matrix describing the free spherical wave propagation of the photoelectron from one site to another, and T_A the diagonal matrix describing the scattering process of the photoelectron spherical wave by the atoms located at the various sites around the photoabsorber. Each χ_n accounts for the partial contribution of the order n, coming from the processes in which the photoelectron has been scattered $n-1$ times by the atoms surrounding the photoabsorber before returning to the origin. χ_2 is the spherical wave single-scattering term and the higher-order terms χ_n probe the n-particle correlation functions. It is possible to show[12,22] that for each n

$$\chi_n^l(k)=\sum_p A(k,R_{ij}^p)\sin[kR_{\mathrm{tot}}^p+\phi_n^l(k,R_{ij}^p)+2\delta_{0l}]\ . \tag{3}$$

Here the sum is over all possible paths of p of order n, starting from and ending at the central atom position with $n-1$ intermediate steps on the surrounding atoms. R_{tot}^p indicates the corresponding total path length and R_{ij}^p are the vectors joining consecutive sites along the path. $A(k,R_{ij}^p)$ and $\phi_n^l(k,R_{ij}^p)$ are amplitude and phase functions. The theory provides well-defined expressions for these quantities,[25] in terms of the phase shifts of the potential. Equation (3) represents the generalization of the EXAFS formula to higher-order terms in the multiple-scattering series. We note that this equation has the same form as the EXAFS formula.

Returning to Si, we have evaluated the phase shifts within the muffin-tin scheme using the usual Mattheiss-Norman criteria.[26] The model potential was a real local potential, with the exchange term treated in the $X\alpha$ approximation. To take into account the inelastic losses we corrected the amplitudes by a phenomenological factor

$\exp(-R_{\rm tot}/\lambda)$ using a mean free path λ close to that obtained from the $2p$ core-level photoemission spectra in the region of interest.[22,25]

Using these phase shifts, we have calculated from Eq. (3) the contribution to the absorption coefficient coming from each particular path present in the structure. Moreover, in order to calculate in a reliable way the observed signal, in such a highly disordered structure, we had to perform the configurational average $\langle \chi_n^l(k) \rangle$ with respect to the distribution function $g(R_{i0})$ of the positions R_i around the reference center R_0 (photoabsorber) ($R_{i0}=R_i-R_0$). In other words

$$\langle \chi_n^l(k) \rangle = \int \prod_{m=1,n-1} d^3R_{m,0} g_n(R_{10},\ldots,R_{n-1,0}) \times \chi_n^l(k,R_{10},\ldots,R_{n-1,0}) ,$$

where $g_n(R_{10},\ldots,R_{n-1,0})$ is the n-body correlation function. This was accomplished using the procedure described in detail elsewhere.[27] As a model for the amorphous structure we used the coordinates of the Wooten, Winer, and Weaire model[4] (hereafter referenced as the WWW model). Using this model we obtained the $g_2(r)$ and the first peak of $g_3(r_1,r_2,\theta)$ correlation functions that are used in the averaged procedure. In Fig. 4 these two functions are depicted. The first peak of $g_3(r_1,r_2,\theta)$ refers to the basic triangle in the tetrahedron, r_1 is the first bond length, r_2 is the second bond length, while θ is the angle between the two bonds. This peak is Gaussian and centered around the c-Si values of 2.35 Å for the distances and 109.47° for the angle. We refer to Ref. 27 for more details.

In Fig. 5(a) we compare the experimental fine-structure signal of the a-Si sample with our calculated $\langle \chi_2^1(k) \rangle$ signal due to only the first coordination shell. The overall good match in the phases gives us confidence of the correctness of the theoretical assumptions made: the slight mismatch in the amplitudes can be accounted for by a mean-free-path correction. In Fig. 5(b) we compare the residual signal with the contribution due to the second-shell EXAFS, calculated in the same way. This latter practically coincides with the total $g_2(r)$ averaged residual signal, the effect of the third and higher shells being negligible due to the dihedral angle distribution. We clearly see that in such case a rather large phase mismatch is present at k values higher than 4 Å^{-1} and that the amplitudes do not match in all the k range.[28] The observed discrepancy is not due to the particular structural model used: in fact, as already emphasized, all the existing theoretical structural models of a-Si well reproduce the experimental pair correlation function and therefore are expected to give similar EXAFS spectra. As a matter of fact, calculations with other theoretical models gave essentially the same result as in Fig. 5(b).

In the light of this evidence we have been forced to consider multiple-scattering corrections as well. Due to the convergence of the series in Eq. (2) and to the washing effect of the configurational average, we retained only the paths $\langle \chi_3^l(k) \rangle$ and $\langle \chi_4^k(k) \rangle$, within the first and the second coordination shells, composed of consecutive first- and second-neighbor bonds.

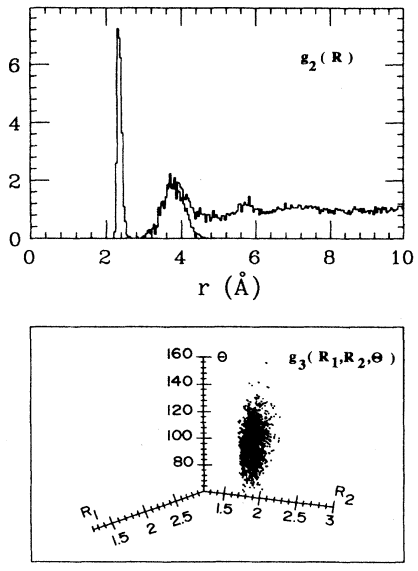

FIG. 4. Graphical view of the $g_2(r)$ and the first peak of $g_3(r_1,r_2,\theta)$ correlation functions obtained using the WWW model. In the histogram for $g_2(r)$ the contribution related to the second shell has been shown explicitly. The distances are in angstroms and the angles in degrees.

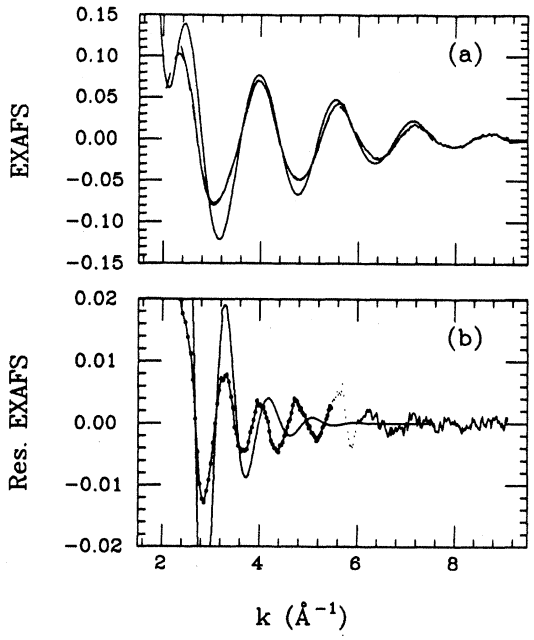

FIG. 5. Comparison between (a) the experimental EXAFS spectrum of a-Si and the calculated first-shell single-scattering contribution for the WWW model, which accounts for most of the signal, and (b) the experimental high-frequency residual and the theoretical single-scattering second-shell contribution.

In Fig. 6 we show the main contributions of the multiple-scattering series besides single scattering. The main $\langle \chi_3^I(k) \rangle$ contribution is due to the χ_{3B} already indicated as a large signal in c-Si.[23] The present calculation, however, shows that several χ_4 contributions are not negligible as well. This is due to the fact that, although these contributions are related to higher terms in the series, they are only marginally affected by the configurational average involving only first-neighbor bonds. It has been verified that other signals due to open paths like χ_{4D} are negligible, as well as the equilateral χ_3 from second-shell neighbors and other possible paths involving third-shell atoms.

From the point of view of the informational content on the correlation functions $g_n(r)$, the signals shown in Fig. 6 are not independent. Many of them are generated by the same feature of a particular g_n and for this reason should be summed together. These sums are shown in Fig. 7. The first peak in the pair correlation function g_2 affects only the χ_{4A} contribution in the high-frequency residual signal.[27] This is the only contribution from the g_2 besides the single-scattering contribution of second shell already shown in Fig. 5(b) and it is indicated as $g_2^{(1)}$ in Fig. 7. Several signals are due to the main peak of the $g_3(r_1,r_2,\theta)$ which is related to the triangle having two first-shell distances as sides and one second-shell distance.[27] This sum is reported in Fig. 7 as $g_3^{(1)}$. These signals are now independent because they are related to different features of the g_n distributions. The main result

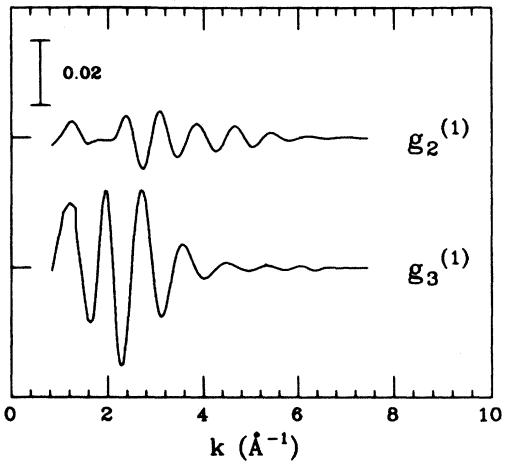

FIG. 7. Total theoretical multiple-scattering contributions in the high-frequency signal associated with the first peak in g_2 and g_3.

of this calculation is that, besides the well-established information on the pair correlation function from the single-scattering terms of the series, a strong signal from the main feature of the g_3 is also expected.

The sum of the contributions coming from the two peaks of the g_2 is compared in Fig. 8(a) with the a-Si residual signal. The agreement remains poor, indicating the need to take into account the contribution coming

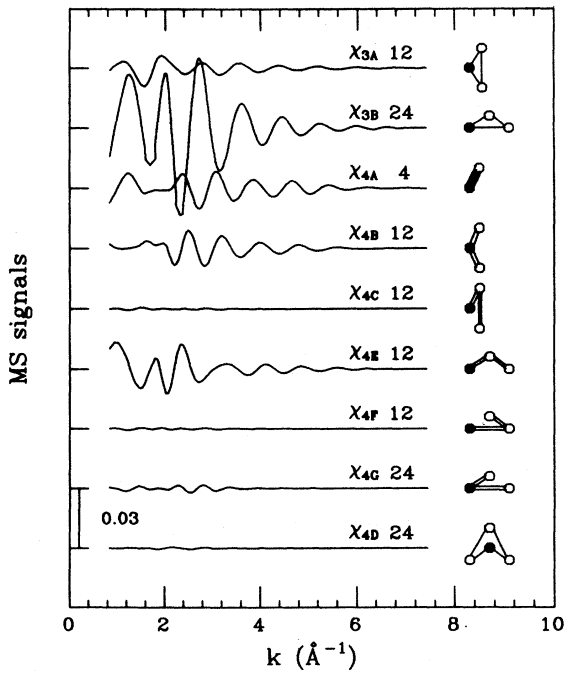

FIG. 6. The main multiple-scattering contributions in a-Si. On top of each signal is reported the conventional name and the degeneracy of the path. The diagrams on the right show the geometrical structure of the path. The photoabsorber is indicated by a solid dot.

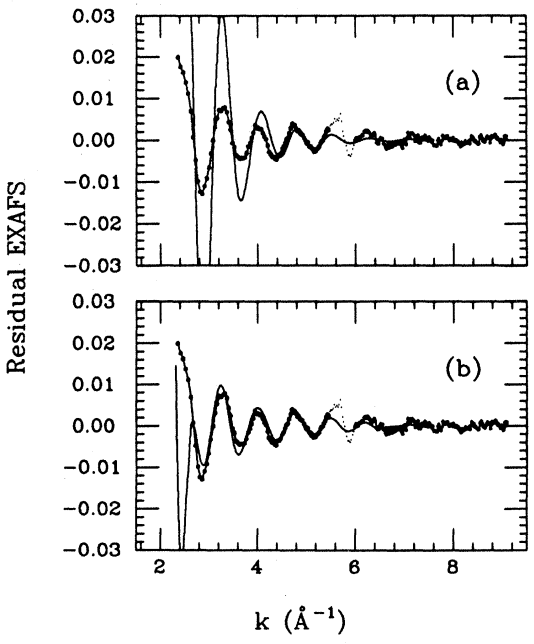

FIG. 8. Comparison between the experimental high-frequency residual of the a-Si sample with (a) the sum of single- and multiple-scattering contributions associated with the first peak in g_2; (b) the sum of all single- and multiple-scattering contributions referred to the WWW model.

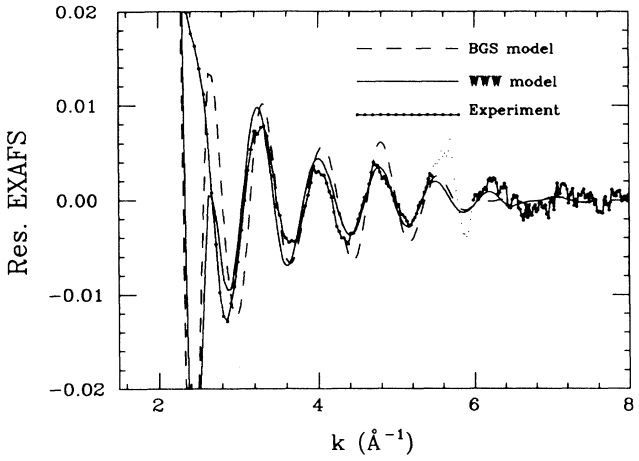

FIG. 9. Comparison among the experimental high-frequency residual signal and two theoretical calculations obtained using the WWW and BGS (dashed line) models.

from the g_3. The comparison with the total single- and multiple-scattering contributions (g_2 signal plus g_3 signal) is shown in Fig. 8(b). The agreement between the calculation and the experiment is now very good both in amplitudes and in phase without any adjustment of the theoretical parameters. It should be noted that the high-k region ($k \geq 5$ Å^{-1}) is mainly dominated by the $g_2^{(1)}(\chi_{4A})$ while the low-k region is affected by the interplay between $g_3^{(1)}$ and second-shell EXAFS.

The structural parameters used refer to the WWW model and no attempt was made to fit the experimental spectrum.

In Fig. 9 we report the comparison among the experimental residual signal and two theoretical signals calculated using the WWW model and the Biswas, Grest, and Soukoulis (BGS) model.[29] As clearly shown the two theoretical signals are quite different both in phase and amplitude and the WWW model gives rise to a calculated signal in better agreement with the experiment. This fact indicates that the total calculated signal is sensitive to the changes in the angular disorder and/or in the correlations obtained by choosing a different structural model. The extraction of reliable structural parameters related to g_3 should then be feasible; however, it lies beyond the scope of this paper.

We emphasize that in order to obtain such a good agreement between theory and experiment a crucial step was to develop a correct way of performing the configurational averages.[27]

V. CONCLUSION

We presented a detailed quantitative characterization of the first coordination shell of *a*-Si and *a*-Si:H using x-ray-absorption spectroscopy. We were able to detect appreciable structural differences among the amorphous samples.

The second important conclusion of the present paper is that, contrary to what is generally believed, XAS can provide structural information beyond the first coordination shell in amorphous materials. It has also been shown that a non-negligible high-frequency contribution is present in x-ray-absorption spectra of *a*-Si besides the first-shell EXAFS. Through multiple-scattering calculations, we have shown that such contribution arises from the second-shell peak of the $g_2(r)$ and from the main peak of the three-body correlation function $g_3(r_1,r_2,\theta)$. To our knowledge this is the first time that effects associated with $g_3(r_1,r_2,\theta)$ are revealed in an x-ray-absorption spectrum of an amorphous system. This occurrence shows that XAS has the potentiality for probing the structural information beyond the pair correlation function in disordered systems. In this way one can discriminate among the various models of amorphous structure at the level of high-order correlation functions.

Finally, the good agreement between the experimental residual signal and the theoretical calculation obtained using the WWW model indicates that this model describes correctly the level of disorder in our *a*-Si sample.

ACKNOWLEDGMENTS

We acknowledge the invaluable support and the interesting suggestions from P. Lagarde and A. M. Flank of LURE. Thanks are also due to C. Coluzza and P. Rudolf for providing us with the *a*-Si sample and to D. Della Sala for the ir measurements. We are grateful to K. Winer for providing us with the coordinates of the WWW models. One of us (A.F.) gratefully acknowledges a grant from the Consorzio dell'Area per la Ricerca (Trieste, Italy).

[1]J. F. Grackzyk, Phys. Status Solidi A **55**, 231 (1979).
[2]W. Schulke, Philos. Mag. B **43**, 451 (1981).
[3]R. Bellissent, A. Chenevas-Paule, P. Chieux, and A. Menelle, J. Non-Cryst. Solids **77&78**, 213 (1985).
[4]F. Wooten, K. Winer, and D. Weaire, Phys. Rev. Lett. **54**, 1392 (1985).
[5]F. Wooten and D. Weaire, in *Solid State Physics,* edited by H. Ehrenreich and D. Turnbull (Academic, New York, 1987), Vol. 40, p. 1.
[6]R. Biswas, G. S. Grest, and C. M. Soukoulis, Phys. Rev. B **36**, 7437 (1987).
[7]N. Tomassini, A. Amore Bonapasta, A. Lapiccirella, K. W. Lodge, and S. L. Altmann, J. Non-Cryst. Solids **93**, 241 (1987).
[8]R. Car and M. Parrinello, Phys. Rev. Lett. **60**, 204 (1988).
[9]D. E. Polk, J. Non-Cryst. Solids **5**, 365 (1971).
[10]G. A. N. Connel and R. J. Temkin, Phys. Rev. **9**, 5323 (1974).
[11]Some reviews are P. A. Lee, P. H. Citrin, P. Eisenberger, and B. M. Kincaid, Rev. Mod. Phys. **53**, 769 (1981); T. M. Hayes and J. B. Boyce, in *Solid State Physics,* edited by F. Seitz, D. Turnbull, and H. Ehrenreich (Academic, New York, 1981), Vol. 37, p. 173; B. K. Teo and D. C. Joy, in *EXAFS Spectroscopy* (Plenum, New York, 1981).
[12]C. R. Natoli and M. Benfatto, J. Phys. (Paris) Colloq. **47**, C8-

11 (1986).
[13]M. Benfatto, C. R. Natoli, A. Bianconi, J. Garcia, A. Marcelli, M. Fanfoni, and I. Davoli, Phys. Rev. B **34**, 5774 (1986).
[14]R. Bellissent, A. Chenevas-Paule, P. Lagarde, D. Bazin, and D. Raoux, J. Non-Cryst. Solids **59&60**, 237 (1983).
[15]A. Menelle, A. M. Flank, P. Lagarde, and R. Bellissent, J. Phys. (Paris) Colloq. **47**, C8-379 (1986).
[16]A. Filipponi, D. Della Sala, F. Evangelisti, A. Balerna, and S. Mobilio, J. Phys. (Paris) Colloq. **47**, C8-375 (1986).
[17]A. Filipponi, E. Bernieri, and S. Mobilio, Phys. Rev. B **38**, 3298 (1988).
[18]P. Eisenberger and B. Lengeler, Phys. Rev. B **22**, 3551 (1980).
[19]B. K. Teo and P. A. Lee, J. Am. Chem. Soc. **101**, 2815 (1979).
[20]P. H. Citrin, P. Eisenberger, and B. M. Kincaid, Phys. Rev. Lett. **36**, 1346 (1976).
[21]E. A. Stern, B. A. Bunker, and S. M. Heald, Phys. Rev. B **21**, 5521 (1980).
[22]A. Bianconi, A. Di Cicco, N. V. Pavel, M. Benfatto, A. Marcelli, C. R. Natoli, P. Pianetta, and J. Woicik, Phys. Rev. B **36**, 6426 (1987).
[23]A. Balerna, M. Benfatto, S. Mobilio, C. R. Natoli, A. Filipponi, and F. Evangelisti, J. Phys. (Paris) Colloq. **47**, C8-357 (1986).
[24]A. Filipponi, Phys. Rev. B **37**, 7027 (1988).
[25]A. Di Cicco, N. V. Pavel, and A. Bianconi, Solid State Commun. **61**, 635 (1987).
[26]L. Mattheis, Phys. Rev. **134**, 4970 (1964); J. G. Norman, Mol. Phys. **81**, 1191 (1974).
[27]M. Benfatto, C. R. Natoli, and A. Filipponi, Phys. Rev. B **40**, 9626 (1989).
[28]In a previous paper (Ref. 22) we have claimed that the second-shell EXAFS accounts for the phase of the residual signal, but that time we were looking at a rather short k range (up to 4.5 Å^{-1}).
[29]R. Biswas, G. S. Grest, and C. M. Soukoulis, Phys. Rev. B **36**, 7437 (1987).